

# Interaction at the barrier in the systems ${}^9,{}^{10},{}^{11}\text{Be} + {}^{209}\text{Bi}$ : Well-established facts and open questions

C. Signorini<sup>a</sup>

Physics Department and INFN, via Marzolo 8, I-35131 Padova, Italy

Received: 1 May 2001

**Abstract.** The experimental data relative to the interaction for the systems  ${}^9,{}^{10},{}^{11}\text{Be} + {}^{209}\text{Bi}$  at the Coulomb barrier are critically discussed and compared also with present theories. The break-up (BU) of the two loosely bound projectiles,  ${}^9,{}^{11}\text{Be}$ , seems to influence the fusion process by “hindering” the fusion cross-sections; but, contrary to expectations, the  ${}^{11}\text{Be}$  halo structure has no influence, since no “enhancement” is evident from the existing data. Attempt to describe simultaneously all the  ${}^9\text{Be} + {}^{209}\text{Bi}$  system data: fusion, elastic scattering and BU, within a coupled-channel (CC) approach is only partly successful. It is important, from a theoretical viewpoint, to include in the CC formalism as well as possible the BU process both to continuum states as well as to unbound resonances. More accurate and well-focused experiments are also necessary to pin down this problem.

**PACS.** 25.70.Jj Fusion and fusion-fission reactions – 25.70.Mn Projectile and target fragmentation – 24.10.Eq Coupled-channel and distorted-wave models

## 1 Introduction

The main goal of the present paper is a critical review and discussion of the various aspects connected to the interaction around the Coulomb barrier in the systems  ${}^9,{}^{10},{}^{11}\text{Be} + {}^{209}\text{Bi}$ . This is based primarily upon the experimental results achieved in several years’ collaboration among groups active in Padova, RIKEN, Napoli, IAE (Beijing), Munich, U.K.; some of these data are not yet published and should be considered as preliminary.

The main characteristics of these three nuclei are the following:

- ${}^{11}\text{Be}$  has a well-established moderate halo structure, is very loosely bound with  $S_n = 0.504$  keV and has  $T_{1/2} = 14$  s. It has been produced up to now as radioactive ion beam (RIB) with  $\sim 10^{+5}$  Hz intensities and poor emittance.
- ${}^9\text{Be}$  is stable, loosely bound with  $S_n = 1.665$  MeV. It has a “Borromean” structure since once the valence neutron is removed the  ${}^8\text{Be}$  core is unbound and breaks into two alphas with  $T_{1/2} = 0.07$  fs. Moreover it is strongly deformed due to its  ${}^8\text{Be}$  core which has a well-known 2-alphas structure.
- ${}^{10}\text{Be}$  is radioactive, but with a very long lifetime  $T_{1/2} = 1.6$  My, and is well bound with  $S_n = 6.7$  MeV. It has been produced up to now as RIB with characteristics similar to  ${}^{11}\text{Be}$ . But its long lifetime makes it a possible candidate for a beam from a conventional accelerator.

The simple theoretical expectations for these nuclei are the following: i)  ${}^{11}\text{Be}$ : the halo, originating also from the small  $S_n$ , means larger radius  $\rightarrow$  smaller Coulomb barrier  $\rightarrow$  larger fusion cross-section; ii)  ${}^{11}\text{Be}$  and  ${}^9\text{Be}$ : the small  $S_n$  suggests large BU cross-sections  $\rightarrow$  smaller fusion cross-section  $\rightarrow$  large absorption cross-section; iii)  ${}^{10}\text{Be}$  is expected to behave “normally”.

All these “simple” theoretical expectations have to be based on more sound theoretical grounds within extended couple-channel (CC) calculations. On these respect crucial point is the choice of the potential to be utilised and how to include the coupling to the continuum BU; in particular this last one is expected to play a crucial role. From an experimental point of view it is important to plan suited and well-focused experiments, since for the immediate future the results with RIB will suffer from statistical accuracy due to the low  ${}^{11}\text{Be}$  beam intensities available.

## 2 The nucleus ${}^{11}\text{Be}$ : what is the influence of its halo structure?

We begin with a comparison of the fusion cross-sections in the systems  ${}^9,{}^{11}\text{Be} + {}^{209}\text{Bi}$  shown in fig. 1 [1,2]. The relative behaviour of the two cross-sections is unexpected. Below the barrier the two cross-sections seem rather similar while any type of simple calculations foresees an enhancement of the  ${}^{11}\text{Be}$  ones if only the halo and not BU is considered. As an example we report the predictions of

---

<sup>a</sup> e-mail: signorini@pd.infn.it

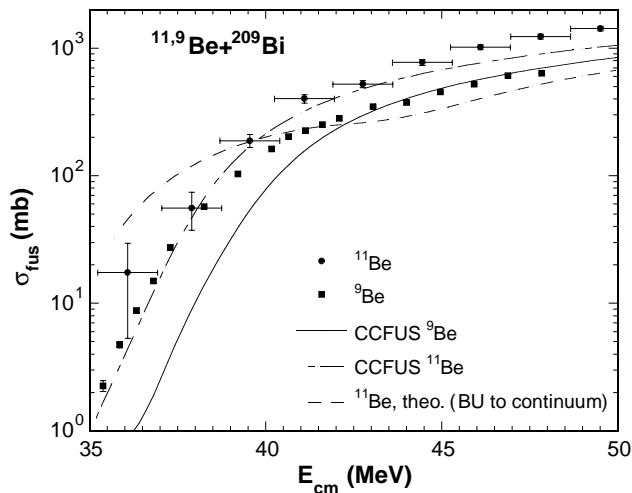


**Fig. 1.** Fusion cross-sections and theoretical predictions. The curve labelled “ $^{11}\text{Be}$ , theo.” is calculated for the system  $^{11}\text{Be} + ^{208}\text{Pb}$  but should not differ too much from the  $^{11}\text{Be} + ^{209}\text{Bi}$  one.

the simple CCFUS code where the halo structure, *i.e.* a larger matter radius, is included. This effect needs anyhow an experimental confirmation since the  $^{11}\text{Be}$  fusion cross-section was obtained [1] as the sum of three channels:  $5n+4n$ +fission. The long-lived  $3n$  one, expected to be relevant below the barrier, could not be measured; this might call for a larger subbarrier fusion cross-section. In addition the fission cross-section could have been overestimated in ref. [1] since it is much larger than in the similar system  $^9\text{Be} + ^{208}\text{Pb}$  [3] and this might call for a smaller fusion cross-section. These two opposite tendencies might as well cancel but this anyhow must be experimentally verified. Indeed a new experiment has already been done at RIKEN and the data are under analysis. This experiment is expected also to verify the cross-sections above the barrier, since the  $^{11}\text{Be}$  ones are larger than the  $^9\text{Be}$  ones beyond any realistic expectation; see *i.e.* the CCFUS predictions in fig. 1.

It is interesting also to compare the  $^{11}\text{Be}$  data with the results of recent calculations [4] which include also coupling to the  $^{11}\text{Be}$  continuum BU. These calculations were done for a  $^{208}\text{Pb}$  target (not for  $^{209}\text{Bi}$ ) and do not intend to predict cross-sections but rather to see a general trend. Anyhow this trend is rather different from the experimental data, since below (above) the barrier the cross-sections are larger (smaller) than the experimental data.

For what concerns the real influence of the  $^{11}\text{Be}$  halo structure we have anyhow to wait for further more accurate data, while the BU aspects can be investigated in detail also with the similar stable nucleus  $^9\text{Be}$ .

### 3 The nucleus $^9\text{Be}$ : well-established facts and open questions

We are studying in detail the  $^9\text{Be}$  reaction dynamics at the barrier since we can measure cross-sections with high

statistical accuracy; this allows to search for possible effects originating from the small binding energy. The same effects are expected to show up also in  $^{11}\text{Be}$  with different weights.

At first we have tried to find whether there is any effect in the barrier distribution; this can be extracted from the fusion cross-section excitation functions according to a well-established procedure. As already mentioned, once the valence neutron is removed from  $^9\text{Be}$ , this nucleus splits into two alphas. The process is an end effect  $^9\text{Be} \rightarrow n+\alpha+\alpha$ . Indeed the break-up fusion with alpha-particles has been reported in the  $^9\text{Be} + ^{208}\text{Pb}$  system [3] and we have verified that this happens also in our system; these alpha-particles feel a lower barrier. But the barrier distribution extracted for both  $^{209}\text{Bi}$  and  $^{208}\text{Pb}$  targets do not show evidence of multiple barriers in the low-energy side as well as in the high-energy one, as we can see from fig. 2.

The analysis of the cross-sections above the barrier with both targets give evidence, from different approaches [2,3], that the fusion cross-sections are reduced by  $\sim 30\%$  with respect to realistic expectations; this could be attributed to the competing BU reaction mechanism with all BU fragments escaping fusion, *i.e.* reducing its cross-section.

These results have stimulated a deeper study of the mechanism of the interaction at the barrier with  $^9\text{Be}$ : namely scattering and reaction cross-section which should bear a signature of BU.

The elastic scattering was measured with accuracy at five energies from 40 to 48 MeV [5]. Figure 3 shows some relevant results of this work. The nuclear potential at the barrier, extracted from the data, has an unusual behaviour, as discussed in detail in ref. [5], and this reflects the existence of strong absorption channels (from BU) at the barrier. These channels are indeed well visible in the spectra of charged particles detected together with the elastic-scattering events; a clear example is shown in fig. 4. The broad structure around 16 MeV was assigned to alpha-particles originating from the disintegration of  $^8\text{Be}$  produced by  $^9\text{Be}$  BU or  $1n$  transfer. This is not an insulated phenomenon; something similar is reported for the system  $^6\text{He} + ^{209}\text{Bi}$  [6],  $^9\text{Be} + ^{208}\text{Pb}$  [7], and recently  $^{6,7}\text{Li} + ^{208}\text{Pb}$  [8]. The excitation function of this “alpha bump” [9] is shown in fig. 5 together with the fusion cross-sections. It is to be underlined how this cross-section is very large below the barrier, while fusion is very small.

Coupled-channel calculations have been done with the code FRESCO in order to explain globally all the  $^9\text{Be}$  data: elastic scattering, fusion, BU. We have included in the calculations all the channels connected, or expected to be connected, to this alpha bump: namely BU and  $1n$  transfer, both producing  $^8\text{Be}$  and consequently alpha-particles. We included therefore the excitation of three  $^9\text{Be}$  levels (all unbound) at 1.68 MeV,  $1/2^+$ ; 2.43 MeV,  $5/2^-$ ; 6.76 MeV,  $7/2^-$  and the reorientation of the  $3/2^-$  g.s.; the three negative-parity states constitute a strongly deformed rotational band. For the transfer we considered the first 7 levels in  $^{209}\text{Pb}$  already observed in the

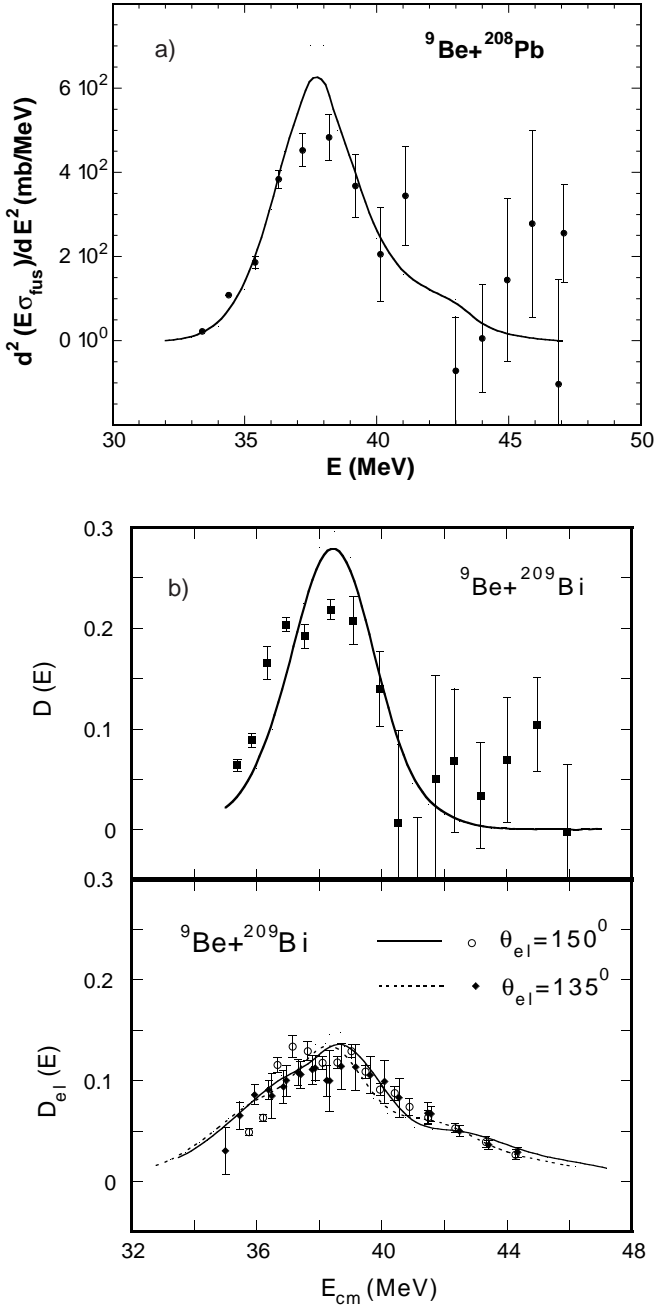


**Fig. 2.** Barrier distributions experimental and theoretical: a)  $^9\text{Be} + ^{208}\text{Pb}$  system from ref. [3], b)  $^9\text{Be} + ^{209}\text{Bi}$  system from our work. The distributions give evidence of only one barrier.

$^{208}\text{Pb}(^9\text{Be}, ^8\text{Be})$  transfer reaction [10]. In this case we have made the reasonable assumption that, in the weak-coupling limit, these levels show up with the same total strength in  $^{210}\text{Bi}$ ; in this nucleus of course the strength is splitted in a multiplet. This approximation allows to reduce significantly the computing time. The seven transfer amplitudes were all assumed to be equal to 1 since all these levels are well known to be of single-particle nature. The potential had a Woods-Saxon shape; the parameters were varied in order to reproduce primarily the elastic-scattering cross-sections [5]. The real potential param-

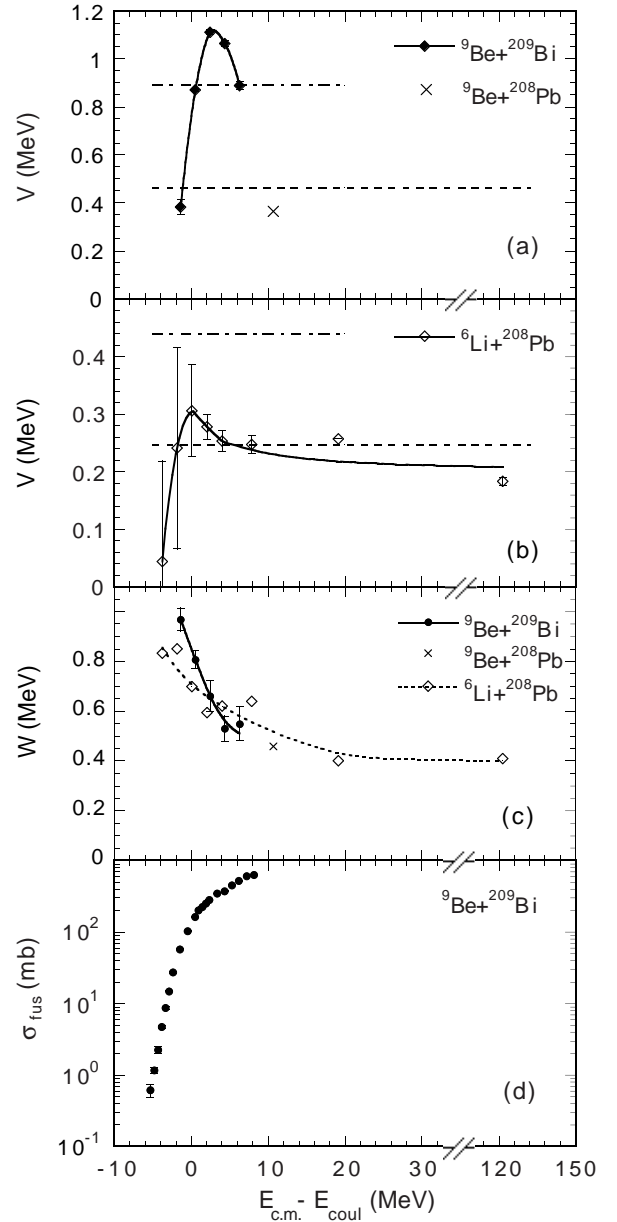


**Fig. 3.** Potential parameters from  $^9\text{Be} + ^{209}\text{Bi}$  elastic scattering calculated at the touching radius  $r_0 = 12.5$  fm. The data from the similar system  $^6\text{Li} + ^{208}\text{Pb}$  are also reported. The curve in (d) shows the fusion cross-section for reference purpose.

eters were varied around the values obtained from the fit to the elastic data reported in ref. [5]. For the imaginary potential parameters we kept  $r_i = 1.0$  fm in order to have absorption inside the nucleus and then we tried to reduce the imaginary depth  $W_i$  as much as possible, since in principle all the couplings included were expected to take into account most of the absorption processes proceeding via specific states or resonances. The parameters reproducing in the best way all the scattering data were the following:  $V_0(W_i) = 175.5(1.5)$  MeV,  $r_0(r_i) = 1.198(1.000)$  fm,  $a_0(a_i) = 0.58(0.68)$  fm. The results of the calculations are

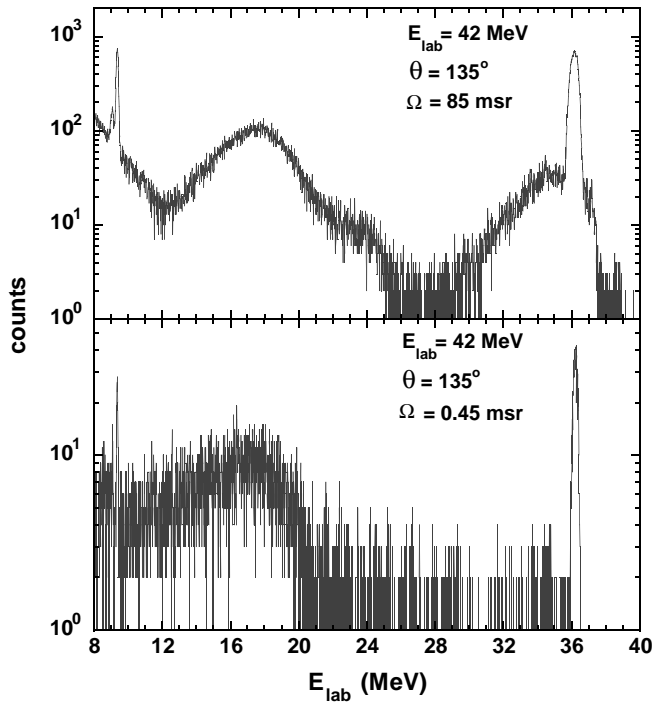


**Fig. 4.** Charged particles spectra observed with different solid angles in the reaction  ${}^9\text{Be} + {}^{209}\text{Bi}$ . The large bump at around 16 MeV is assigned to alpha-particles produced most likely by the  ${}^9\text{Be}$  BU.

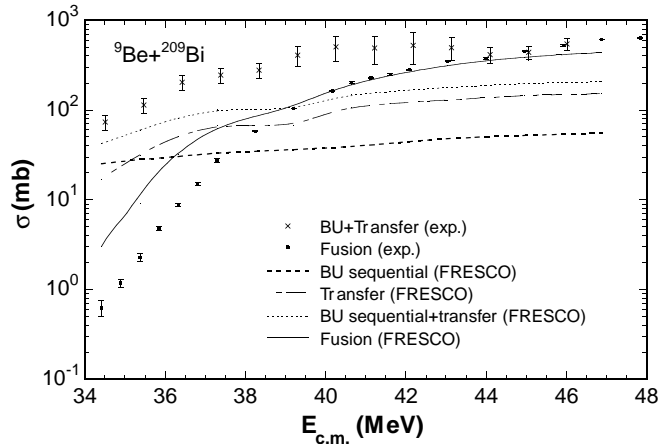


**Fig. 5.** Reaction  ${}^9\text{Be} + {}^{209}\text{Bi}$ ; cross-sections for the production of alpha-particles (most likely originating from BU + 1n transfer) and for the fusion process. The relative theoretical predictions are also drawn.

shown in fig. 6; as we can see all the five angular distributions are well reproduced. The calculations have an oscillatory behaviour at 48 MeV; this originates from the shallow imaginary potential in connection with the procedure for solving the system of second-order differential equations. With a much deeper real potential, but with the same radial behaviour  $V(r)$  in the outer nuclear region ( $V_0 = 400.0$  MeV,  $r_0 = 1.1377$  fm,  $a_0 = 0.572$  fm) the oscillations are practically eliminated; the experimental data are still reproduced even if the agreement is slightly worse

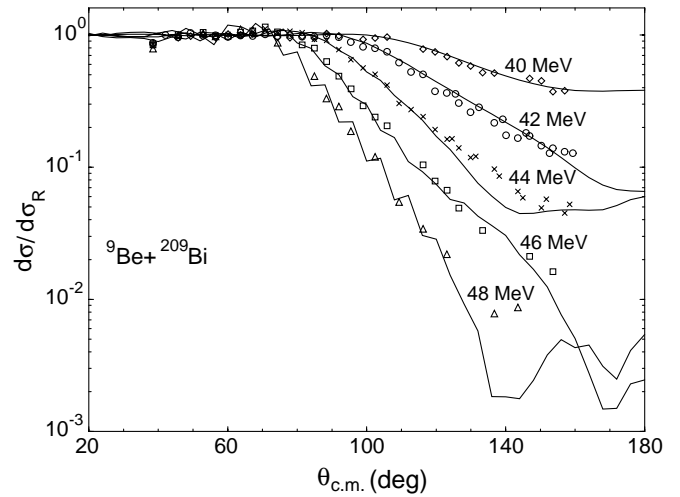


**Fig. 6.** Elastic-scattering cross-sections experimental and theoretical.

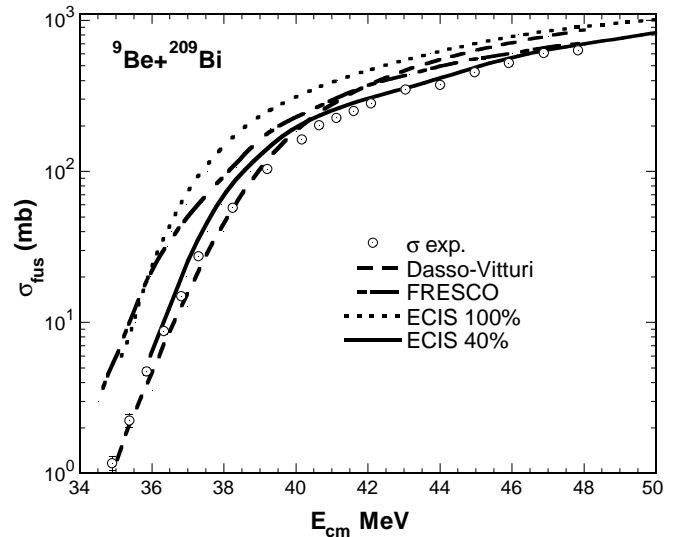


**Fig. 7.** Theoretical calculations for the fusion cross-sections in the system  ${}^9\text{Be} + {}^{209}\text{Bi}$  compared with the experimental data.

than with the original set of potential parameters. The predicted fusion cross-sections are shown in fig. 5 together with the experimental data; the calculations overestimate the cross-sections. We believe that this is due to the non-inclusion of the continuum BU. A better agreement is expected from the inclusion of this additional channel(s) on the basis of several works going on the reaction dynamics of loosely bound RIBs; we are also working on this subject in order to better understand the data. Finally in fig. 7 we are comparing the various calculations done for the fusion cross-sections in the system  ${}^9\text{Be} + {}^{209}\text{Bi}$ .

The curve labelled Dasso-Vitturi which well reproduces the subbarrier region is from ref. [2]; in these CC calculations one general BU channel is considered, the potential parameters were adjusted (and subsequently scaled) in order to reproduce the fusion cross-sections in the neighbouring system  ${}^{16}\text{O} + {}^{208}\text{Pb}$ , where BU phenomena should be negligible.

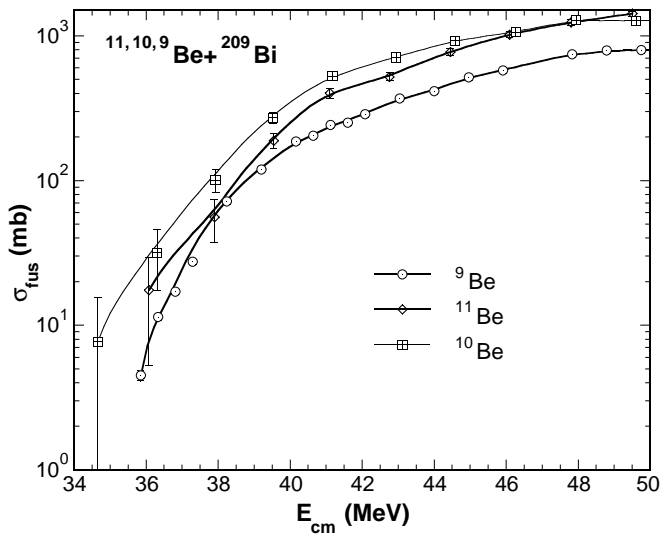


**Fig. 8.** Fusion cross-sections in the systems  $^{11,10,9}\text{Be} + ^{209}\text{Bi}$ . The  $^{11}\text{Be}$  data do not have error bars for the beam energy, differently from fig. 1, because they are the same as for the  $^{10}\text{Be}$  data, since they are measured during the same experimental run. The lines are drawn to guide the eye.

The two curves labelled ECIS are calculated within a CC approach by Alamanos *et al.* [11]: in this case the real part of the potential was obtained by folding realistic mass distributions with the nucleon-nucleon BDM3Y1 interaction. The imaginary potential simulated the incoming wave boundary condition and the  $^9\text{Be}$  excited state at 2.43 MeV was included. But in order to get a good agreement with the data the real potential depth had to be reduced empirically of 40% (curve ECIS 40%).

It is not so clear which is the best approach; in our opinion the question is still open. In fact if from one side the two empirical approaches “Dasso-Vitturi” and “ECIS 40%” seem to better reproduce some portions of the fusion cross-sections, we do not know how they reproduce the elastic scattering which is the most crucial test. Our approach based on the FRESCO code has the ambition of being more fundamental since on the basis of experimental coupling strengths it wants to reproduce simultaneously fusion, scattering and BU/transfer.

#### 4 The nucleus $^{10}\text{Be}$ : is it the good reference one?

Due to the anomalies observed with both  $^{11}\text{Be}$  and  $^9\text{Be}$  nuclei, we decided to analyse also the  $^{10}\text{Be} + ^{209}\text{Bi}$  system which was also measured in the experiment of ref. [1] with limited statistical accuracy. The nucleus  $^{10}\text{Be}$  has no halo and is well bound with consequently no BU effects; this nucleus is therefore expected to behave “normally” and to be a good reference one. The fusion cross-sections in the systems  $^{11,10,9}\text{Be} + ^{209}\text{Bi}$  are shown in fig. 8. The comparison between  $^{10}\text{Be}$  and  $^{11}\text{Be}$  is quite significant since

both data were collected and analysed in the same way; so that most likely all the systematic uncertainties, previously mentioned for  $^{11}\text{Be}$ , can be neglected. Moreover the beam energy spread, of around 1.7 MeV as shown in fig. 1, can be ignored for this relative comparison since it influences in the same way both systems. Above the barrier the  $^{11}\text{Be}$  cross-sections are slightly smaller than the  $^{10}\text{Be}$  ones; this suggests that there are moderate BU effects with both fragments from  $^{11}\text{Be} \rightarrow ^{10}\text{Be} + n$  escaping fusion. But below the barrier the  $^{10}\text{Be}$  cross-sections seem to be definitely larger than the  $^{11}\text{Be}$  ones; this suggests no halo effect and again significant BU effects.

The problem connected to the fact that the  $^9\text{Be}$  cross-sections well above the barrier seem to be too small, or the  $^{10,11}\text{Be}$  ones too large, is still open.

## 5 Conclusions

The most significant conclusion we can draw for the moment, from the comparison of the various experimental data, is that most likely the halo structure has no specific influence on the fusion process contrary to BU which definitely seems to more or less reduce the fusion cross-sections. It would be important anyhow to get more accurate fusion cross-sections with the two RIB nuclei  $^{11,10}\text{Be}$ . It would be also important to measure the noninclusive, pure BU, cross-section at least for  $^9\text{Be}$  projectile:  $^9\text{Be} \rightarrow ^8\text{Be} + n$ .

From a theoretical point of view it seems that the most relevant renormalization of the fusion cross-sections, with weakly bound-halo RIB nuclei, originates from the BU phenomena which proceed mainly via continuum states. It is therefore important to include correctly these channels in the CC calculations.

## References

1. C. Signorini *et al.*, Eur. Phys. J. A **2**, 227 (1998).
2. C. Signorini *et al.*, Eur. Phys. J. A **5**, 7 (1999).
3. M. Dasgupta *et al.*, Phys. Rev. Lett. **82**, 1395 (1999).
4. K. Hagino, A. Vitturi, C.H. Dasso, S.M. Lenzi, Phys. Rev. C **61**, 037602 (2000).
5. C. Signorini *et al.*, Phys. Rev. C **61**, 061603(R) (2000).
6. E.F. Aguilera *et al.*, Phys. Rev. Lett. **84**, 5058 (2000); J.J. Kolata, this issue, p. 127.
7. Australian National University, The Department of Nuclear Physics Annual Report 1998, Canberra ACT 0200, Australia, p. 85.
8. C. Signorini *et al.*, Eur. Phys. J. A **10**, 249 (2001); G.R. Kelly *et al.*, Phys. Rev. C **63**, 024601 (2000).
9. C. Signorini *et al.*, *Proceedings of the International Conference BO2000, Bologna Italy, May 2000*, edited by G.C. Bonsignori *et al.* (World Scientific, Singapore, 2001) p. 413.
10. D.P. Stahel *et al.*, Phys. Rev. C **16**, 1436 (1988).
11. N. Alamanos *et al.*, *Proceedings of the International Workshop on Fusion Dynamics at the Extremes, May 2000, Dubna, Russia*, edited by Yu.Ts. Oganessian, V.I. Zagrebaev (World Scientific, Singapore, 2001) p. 327.